arXiv:1304.6311v1 [math-ph] 23 Apr 2013

Unraveling Self-similar Behavior and Periodicity in the Bouncing Ball through Wavelets

Abhinna Kumar Behera,[1] A. N. Sekar Iyengar,[2] and Prasanta K. Panigrahi[1]

[1]*Department of Physical Science, Indian Institute of Science Education and Research - Kolkata,*
Mohanpur, P.O.- B.C.K.V. Main Office, West Bengal - 741252, India.
[2]*Plasma Physics Division, Saha Institute of Nuclear Physics - Kolkata, 1/AF, Bidhannagar, Kolkata-700064, India.*

The non-stationary dynamics of a bouncing ball comprising of both periodic as well as chaotic behavior, is studied through wavelet transform. The multiscale characterization of the time series discloses clear signature of self-similarity and periodicity. The scale dependent variable window size of the wavelets aptly captures both the transients and non-stationary periodic behavior. The optimal time-frequency localization of the continuous Morlet wavelet is found to delineate the scales corresponding to different periodic modulations. Self-similar behavior is quantified by the generalized Hurst exponent, obtained through both wavelet based multifractal detrended fluctuation analysis and Fourier methods. The discrete Daubechies basis set has been applied for detrending the temporal behavior to reveal the multifractal character underlying the dynamics.

Keywords: Wavelet based multifractal detrended fluctuation analysis (WBMFDFA), Morlet wavelet, Daubechies4 (Db4), Scaling exponent, Fractal dimension, Hurst & Lyapunov exponents.

INTRODUCTION

Driven non-linear systems are well known to exhibit complex dynamics, ranging from stable to unstable periodic motions and chaotic behavior, under different conditions [1-4]. A number of simple systems e.g., coupled pendulum, electrical circuits can reveal extremely complex dynamics [1]. Well known systems such as bilinear oscillator [5], billiards [6-7], Chua circuit [8-9] have been studied quite extensively in the literature. More complex systems like impact oscillators reveal highly complex dynamical behavior, as certain periodic orbit of the system goes through grazing and enters the impacting regime [5]. Quantization of the Sinai billiard, a two dimensional stochastic and ergodic system, has been studied extensively. Bifurcations in the periodic orbit of classical dynamical systems e.g., quartic oscillator, have been shown to have effect on the quantal dynamics [10]. All these make exploration of classical non-linear systems, an exciting area of ongoing research.

The non-linearity in these systems can arise from non-linear interactions or from imposed boundary conditions. In linear cases, the driving force can induce modulations to commensurate with the driving frequency, whereas in the case of non-linearity, other frequencies can manifest. Here, we explore the rich dynamics of the driven ‘ Bouncing ball ’ system and characterize its complex temporal behavior through Fourier method and wavelet based approach. This system has been studied earlier due to its interesting dynamics. Tufillaro et al., illustrated the period doubling route to chaos in such systems in the presence of dissipation [11-12]. They used frequency and amplitude as controlling parameters to demonstrate the curves in parameter space that separate periodic orbits. Heck et al., used high speed camera for observing the dynamics which was then modeled numerically [13]. Kini et al., configured a computer controlled system in order to ascertain the state of the bouncing ball system more accurately [14]. A. Okninski et al. have studied numerically as well as analytically the dynamics of a bouncing ball moving in a gravitational field and colliding with a vertically moving table with constant velocity [15].

We identify and locate the time varying periodic components, as well as quantify the chaotic dynamics through wavelets. This driven system shows non-stationary behavior and unstable periodic orbits. It also exhibits chaotic dynamics under appropriate parametric conditions. We make use of both continuous and discrete wavelets to characterize the periodic as well as self similar behavior of this system [16]. The periodic components are ascertained by isolating the variations in both temporal and frequency domains. Morlet wavelet, a product of a variable Gaussian window and a sinusoidal function, is used to identify local periodic modulations. Wavelet transform splits the input time series into components that depend on position and scale. One then characterizes the variations in it, by changing the scale for a particular location. We determine the multifractal scaling properties through wavelet based detrended fluctuation analysis [17].

Materials and Methods

Set up: A loud speaker was connected to a function generator, a cathode ray oscilloscope and a resistor. A piezoelectric film was set properly on the base of the speaker to prepare the platform for the ball to bounce [12, 18]. Input frequency of the function generator was set to $49Hz$ and was made to generate a sinusoidal potential, $V = V_0 sin(\omega t)$. Fig.1 depicts the experimental set up and Fig.2 shows a typical potential time series. The ‘Denoised’ version of the raw signal is shown below it. For each input voltage V_0, the frequency input ω is varied from $25Hz$ to $100Hz$, in the step size of $15Hz$. This process was repeated for $10V, 20V, 30V$ and $40V$ input voltages. The potential fluctuations of the piezoelectric crystal due to the bouncing of the ball above it, is the time series to be analyzed in the following sections.

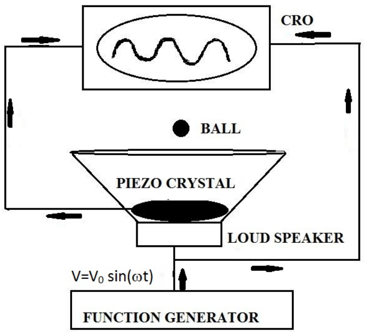

FIG. 1: Schematic illustration of the experimental setup.

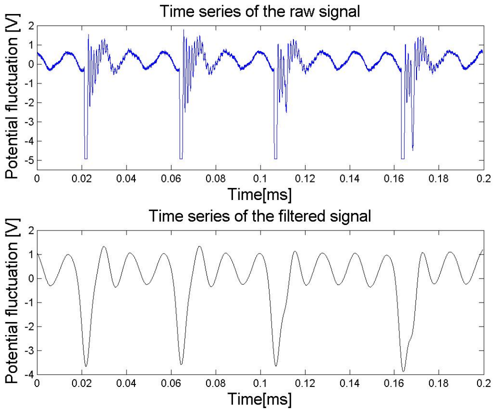

FIG. 2: The potential time series of the bouncing ball with the corresponding filtered one shown below it. The signal is for forcing parameter values of 40V and 70Hz.

The bouncing ball shows periodic behavior for smaller values of the forcing parameters. For higher values of the potential, the time series exhibits intermittency [18]. It shows short-time periodic behavior and time varying transient dynamics. As the forcing frequency increases with constant forcing voltage, the ball shows non-linear behavior [14].

ANALYSIS OF THE BOUNCING BALL MOTION

Lyapunov Exponent

We start with the estimation of the Lyapunov exponent (λ). For certain low values of forcing parameters, it is found to be negative. As is well known, negative Lyapunov exponents are characteristic of dissipative systems. These systems exhibit asymptotic stability. Hence for negative λ, the orbit attracts to a stable fixed point or stable periodic orbit. The more negative the exponent, the greater the stability. We also find that the bouncing ball system shows periodic behavior for small forcing parameters [19]. For higher values of the forcing parameters, $\lambda > 0$ is obtained. In this domain, the system exhibits chaotic dynamics. We note that, even for low potential input, at high frequencies the system's λ is found to be positive.

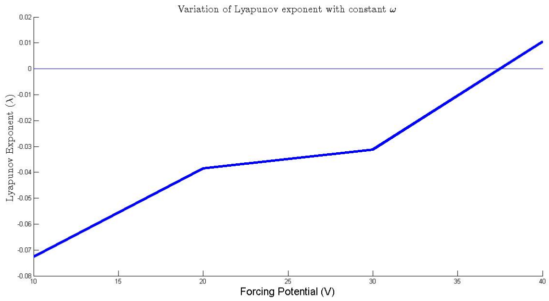

FIG. 3: Variation in the Lyapunov exponent with constant forcing frequency, is shown as a function of forcing potential. The horizontal line corresponds to zero value of the Lyapunov exponent. These λ values are obtained for 70Hz, forcing parameter.

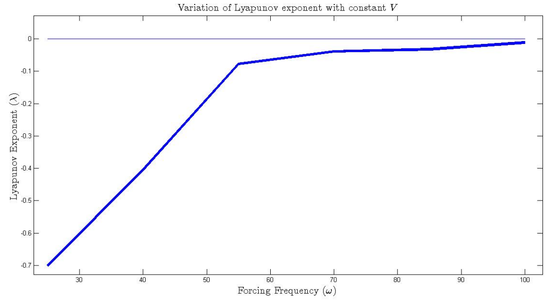

FIG. 4: Variation in the Lyapunov exponent with forcing potential constant, is shown as a function of input frequencies. The horizontal line corresponds to zero value of the Lyapunov exponent. These λ values are obtained for 20V, forcing parameter.

Figs.3 and 4 depict the Lyapunov exponents obtained for varying both the forcing parameters. We now explore in more detail the dynamics of the potential time series. This is done using Fourier method and Wavelet transformation.

Frequency Domain Fourier Analysis

FFT spectrum analyzer in vibrating dynamics is well known to measure frequency response of vibration or shock data. Fourier transform works by decomposing a signal to complex exponential functions of different frequencies [20]:

$$X(f) = \int_{-\infty}^{\infty} x(t) e^{-2\pi i f t} dt \qquad (1)$$

and

$$x(t) = \int_{-\infty}^{\infty} X(f) e^{2\pi i f t} df, \qquad (2)$$

where f and t are frequency and time variables.

Window-based finite impulse response filter and zero-phase digital filter have been used to remove noise, corresponding to the high frequency fluctuations. Fig.5 shows the FFT corresponding to the filtered signal, with its unfiltered counter part.

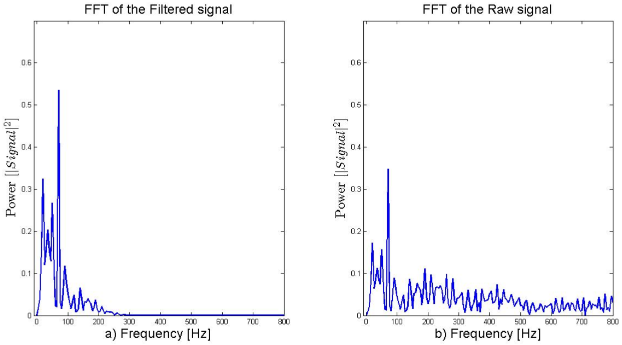

FIG. 5: FFT of filtered and raw signals are shown in 5a and 5b respectively.

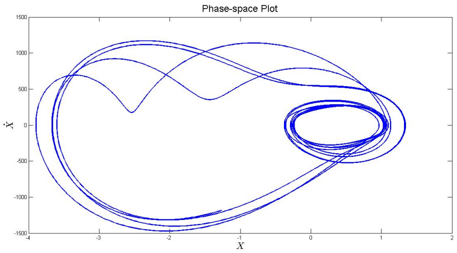

FIG. 6: Phase-space plot corresponding to the denoised version of the signal, is clearly showing periodic motion.

It is noticed that the noise strength in this time varying physical system, increases with increasing magnitude of the forcing parameters. The higher the magnitude of the frequencies present in the signal, the longer time it persists. As mentioned earlier, we have applied a filter on the signal, which removes some initial as well as final transients to clearly observe the periodic behavior in the phase-space [5]. Fig.6 depicts the phase-space plot of the filtered signal, which clearly shows the periodic dynamics. The number of converging loops show that the system has multiperiodicity.

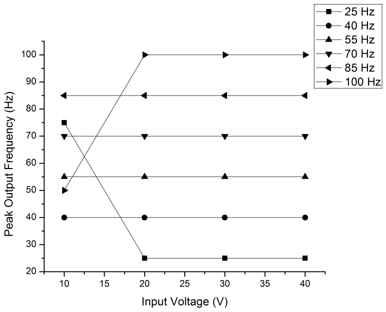

FIG. 7: The power of the maximum output frequencies are shown for each input voltage to the system.

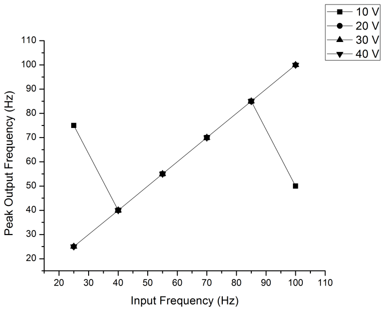

FIG. 8: The power of the maximum output frequencies are depicted for each input frequency.

We now study the output from the system in order to identify the parameter values corresponding to the non-linear motion. Figs.7 and 8 represent the response of the system to varying forcing parameters, with the other one kept constant. In all signals, except for the input parameter of 10V, the highest frequency is same as the respective forcing frequencies indicating linear behavior. For 10V forcing potential, the highest response frequency, output is found to be 75Hz and 50Hz for 25Hz and 100Hz input respectively. For all other forcing parameters, the output response behaves linearly. For high values of forcing parameters, chaotic behavior is observed from the frequency response. The frequency response, gets minimized due to dissipation of the system and also gets amplified for smaller values of forcing parameters. This clearly shows non-linear behavior [14].

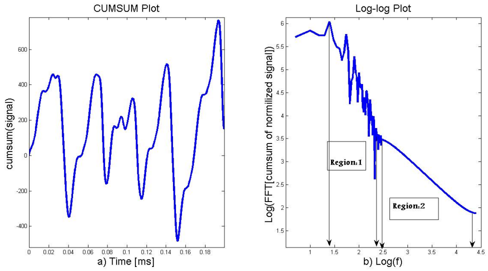

FIG. 9: [9(a)] Cumulative sum of the normalized profile and [9(b)] log-log plot of the FFT the corresponding profile are shown for 40V and 55Hz, forcing parameters.

We now analyze the self-similar behavior of the time series. For this purpose, the 'random walk' is calculated from the cumulative sum of the normalized profile of the system [20]. Fig.9a shows the resulting time series, that reveals the fluctuation characteristic including its periodic components. Fig.9b depicts log-log plot of the FFT of the cumulative sum of the normalized profile, which exhibits power law behavior [21], with varying exponents according to the forcing parameters. The Hurst parameter is estimated from the Fourier power law analysis, based on the monofractal hypothesis and gives the power law exponent β which is related to the Hurst exponent H by $|\beta| = 2H + 1$ [20, 22-23]. It is observed that there are more than one exponent in the power law domain. They are calculated as $\beta_1 = 2.5526$ and $\beta_2 \approx 1$, implying that $H \approx 0$ in the second domain for 40V and 55Hz forcing parameters. In the first domain, persistence is observed; whereas the second domain, corresponding to the high frequency range of $330Hz$ to $25000Hz$, indicates the possible presence of $\frac{1}{f}$ behavior [25-26]. This structure shows the presence of multifractality in the system, which can be estimated using the method like MFDFA [17].

As is well known, fractals can be subdivided in parts, which are a reduced copies of the whole system. They are characterized by their fractal dimension D [27], which is a non-integer number that quantifies the density of fractals in the metric space. The number D measures the degree of fractal boundary fragmentation i.e., irregularity over multiple scales.

The fractal behavior of the signal can be inferred as follows:

$$D = \begin{cases} \frac{7-\beta}{2}, \beta > 3 \\ \frac{5-\beta}{2}, 1 < \beta < 3 \\ \frac{3-\beta}{2}, \beta < 1 \end{cases} \tag{3}$$

In bouncing ball system, the value of D varies in between 1 to 2, depending upon the forcing parameters. We now make use of wavelet transformation for a better understanding of the local dynamics.

Wavelet Based Multifractal Detrended Fluctuation Analysis [WBMFDFA]

Wavelet analysis employs one series of different wavelet functions, which may consist of step functions instead of sine and cosine functions, derivative of Gaussian functions or a multipeak Morlet wavelet, composed of a sine wave multiplied with a Gaussian window. Discrete wavelet basis set is composed of a scaling function, mother and daughter wavelets, and has a strictly finite extent [28].

A convolution product of the data sequence (a function $f(x)$, where x is usually a time or space variable) with the scaled and translated version of the wavelet function as, $\psi(x)$, is known as Wavelet transform. Two parameters are used to perform scaling and translation; the scale parameter s stretches (or compresses) the wavelet to the required resolution, while the translation parameter b shifts the reviewing wavelet to the desired location [29]:

$$(Wf)(s,b) = \frac{1}{s}\int_{-\infty}^{\infty} f(x)\psi^{*}(\frac{x-b}{s})dx \tag{4}$$

where s, b are real as $s > 0$. The wavelet transform acts as a microscope: it uncovers finer details while operating at smaller scales [16].

Discrete Wavelet Transform (DWT)

We have used discrete wavelets belonging to the Daubechies family to remove local polynomial trends from the profile. Considering $x_i (i = 1, 2, 3, ..., N)$ to be the time series of data length N, the 'profile' $Y(t)$ is the cumulative sum of series after subtracting the mean:

$$Y(i) = \sum_{t=1}^{i} [x_t - < x >], i = 1, 2, 3, ...N \tag{5}$$

Next, wavelet transform on the profile Y(t) has been implemented to separate the fluctuations from the trend. The fluctuation extraction involves a wavelet decomposition using the Db4 wavelet. For Db4, in addition to the defining relation $\int \psi_{ji} dt = 0$; the wavelets satisfy the vanishing moment condition $\int t\psi_{ji} dt = 0$. This implies that for a linear signal of the type $y = at + b$, the wavelet coefficients will be zero. Therefore, this linear trend will be captured by the scaling function [16, 21].

The profile series can be decomposed for the Db4 as

$$Y(t) = \sum_{i=-\infty}^{\infty} c_i \phi_i(t) + \sum_{j\geq 0} \sum_{i=-\infty}^{\infty} d_{ij}\psi_{ij}(t) \tag{6}$$

where, $\psi_{ij}(t)$ are wavelet functions of $Db4$ and $\phi_i(t)$ is the father wavelet. The coefficients c_i, d_{ij} are known as the low pass and high pass coefficients. The profile is reconstructed at a particular level i, by taking only the low pass coefficients to extract the trend at level i. This trend is subtracted from the profile to obtain the fluctuations at each scale. Due to the convolution errors, these obtained fluctuations can have edge artifacts, which are removed by performing this fluctuation extraction on the reversed profile and taking the average. After that we subdivide the fluctuations in to n_s non-overlapping segments, such that $n_s = [N/s]$, where the segment length s is related to the wavelet scale i by the number of filter coefficients used in the wavelet. The q^{th} order fluctuation function, $F_q(s)$ is obtained as follows [17]:

$$F_q(s) = \left[\frac{1}{2M_s}\sum_{b=1}^{2M_s}\left[F^2(b,s)\right]^{q/2}\right]^{1/q}, \tag{7}$$

Here q can take both positive and negative integral values. If the time series possesses fractal behavior, then $F_q(s)$ exhibits a power-law scaling,

$$F_q(s) \sim s^{h(q)}, \tag{8}$$

For $q < 0$, $h(q)$, the generalized Hurst exponent, captures the scaling properties of the small fluctuations, whereas for $q > 0$, it captures the large fluctuations. $q = 0$, leads to divergence of the scaling exponent. In that case, logarithmic averaging has to be used to find the fluctuation function;

$$F_0(s) = exp\left[\frac{1}{2M_s}\sum_{b=1}^{2M_s} ln\left[F^2(b,s)\right]^{q/2}\right]^{1/q} \tag{9}$$

For mono-fractal time series, the $h(q)$ values are independent of q. For multifractal time series, $h(q)$ depends on q. The correlation behavior is characterized from the Hurst exponent $(H = h(q = 2))$, which varies from $0 < H < 1$ [23-24].

RESULT

Multifractal behavior of the system

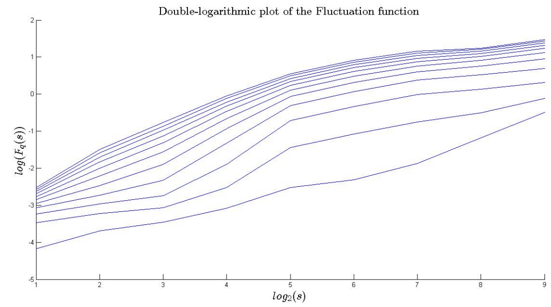

FIG. 10: Log-log plot for the fluctuation function $F_q(s)$ vs. s for various values of q. This plot is for a signal having 40V and 70Hz as forcing parameters.

Fig.10 depicts the *Double-logarithmic* plot of the fluctuation function $F_q(s)$, for q between -10 to 10 in the ascending order.

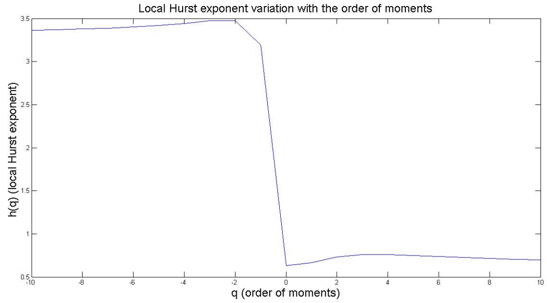

FIG. 11: The multifractal behavior of the spectrum of the bouncing ball is shown. The dependence of the generalized Hurst exponent $h(q)$, as a function of the order of the moment (q), is shown. The signal is for 70Hz and 40V as forcing parameters.

Table.1 shows the Hurst exponents obtained through DWT for different forcing parameters.

TABLE I: Hurst exponents obtained for potential time series using Db4 wavelet

Hurst exponents for varying forcing parameters				
Frequency (Hz)	Potential (V)			
	10	20	30	40
25	0.1981	0.0543	0.1090	0.5153
40	0.4652	0.2609	0.5429	0.6644
55	0.5806	0.5999	0.6778	0.7083
70	0.6286	0.6613	0.7116	0.7338
85	0.2860	0.7235	0.7173	0.7334
100	0.3466	0.6888	0.7171	0.7344

The tabulated data explicitly shows that, the Hurst exponents depend on the forcing parameters. Some values of the Hurst exponent decrease for high forcing parameter with the other one at lower values. It increases with the high values of both the forcing parameters and vice versa. None of these multifractal trends could be gleaned using the Fourier analysis, where one can only qualitatively predict the overall nature of the self-similar behavior. Figs.10 and 11 depict the common nature of the Fluctuation functions and the generalized Hurst exponent respectively. It is found that for high values of the forcing parameters, our system shows persistence.

We now proceed to analyze the periodic behavior through continuous wavelet transform (CWT). Both non-stationary periodic dynamics and the stationary ones clearly manifested in the scalogram of the CWT. We have used Morlet wavelet having optimal time-frequency localization. For a clearer identification of the periodic components, we removed the high frequency fluctuations through the Db4 basis. We have checked that the periodic components are not influenced in the process [26-27].

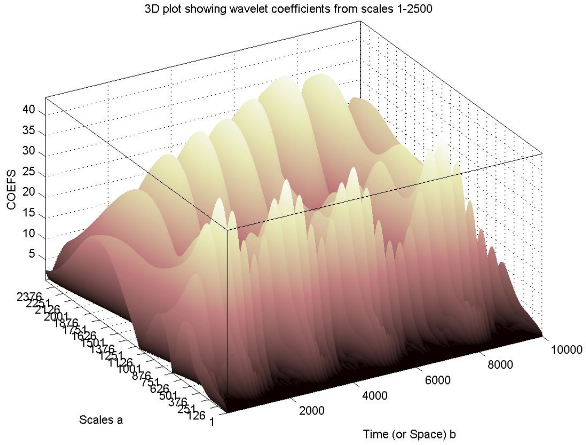

FIG. 12: $3D$ plot of CWT coefficients with time and scale axis, with 40V and 70Hz as forcing parameters. Periodic behavior can be observed from these coefficients at certain scales.

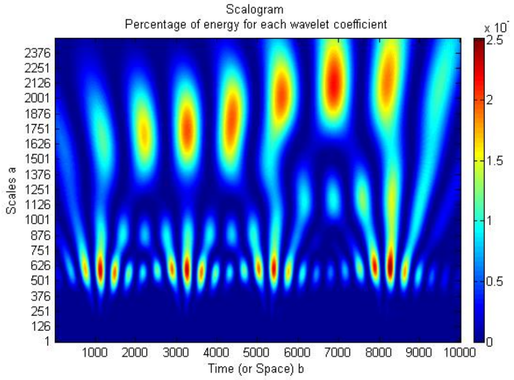

FIG. 13: Scalogram showing energy for each wavelet coefficients, with 40V and 70Hz as forcing parameters.

Morlet wavelet clearly brings out different periodic components in the data sets, as seen in the scalograms given in Fig.12 in a 3D plot. Fig-13 shows the scalogram of the potential time series, presenting the energy of the wavelet coefficients [28-29].

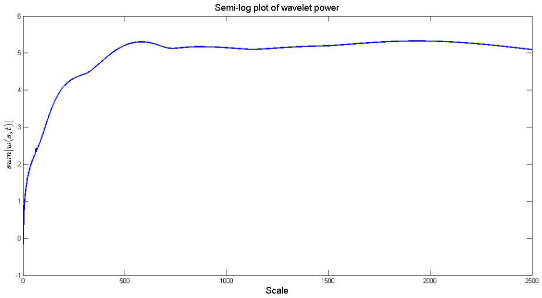

FIG. 14: Semilog plot of wavelet power, summed over all time at different scales. It can be inferred that, the ball has periodicity of 256ms and 579ms, corresponding to 40V and 70Hz forcing parameters.

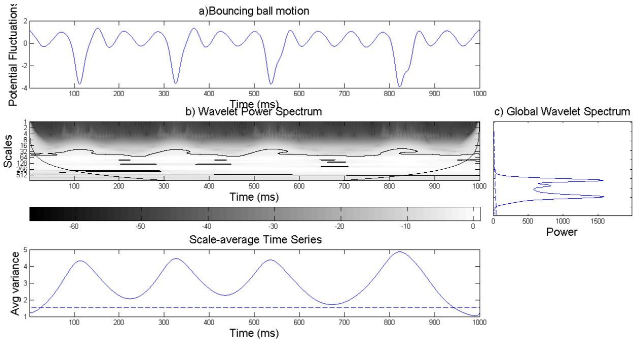

FIG. 15: Wavelet power spectrum with the cone of influence (15b) for the signal (15a) having 40V and 70Hz as forcing parameters. The wavelet analysis can clearly distinguish the two dominant periods of the time series with the confidence level of 95%. Image colors are a representation of the Wavelet Power Spectrum (WPS) normalized by variance. The x-axis shows time; the logarithmic y-axis shows the wavelet scale.

From Figs.13 and 14, it is evident that there are two dominant periods. Fig.15 depicts the wavelet power spectrum including the global wavelet spectrum and the average variance with time. The inset in Fig.15b clearly shows the presence of two periods in the potential time series. In the regions of higher power (the white regions), the dark spots inside the cone of influence, correspond to the periods of $256ms$ and $579ms$ with 95% confidence level [29-30]. These periods compare well with the ones obtained through FFT earlier.

CONCLUSION

In conclusion, we have studied the dynamics of a bouncing ball, a simple driven system exhibiting complex dynamics, which is controlled by the potential and frequency of the driving source. Depending on the driving parameters, it shows self-similar and periodic behavior, which are studied using the Fourier domain analysis and Wavelet transform. It is observed that the potential time series shows a long term switching between high and low frequency values in adjacent pairs. The characterization of the self-similarity revealed multifractal behavior. Wavelets belonging to the Daubechies family optimally removed the local trends of the time series, from which the multifractal character has been reliably extracted. The continuous Morlet wavelet localized the periodic components, which revealed the linear and non-linear behavior. It is quite evident that the bouncing ball system provides an excellent experimental tool to study nonlinear dynamics and chaos. The apparatus can be used to study the complex chaotic or periodic motions, depending on the parametric conditions of the ball.

In future, we would like to analyze the $\frac{1}{f}$ dynamics in more detail. We would also like to model the observed dynamics and explore the possibility of using this system to generate different random matrix ensembles [31-35].

[1] 'Non-linear Dynamics and Chaos' by S. H. Strogatz, Advance Book Program, Perseus Books, Massachusetts (1994).

[2] I. V. Barashenkov and E. V. Zemlyanaya, Phys. Rev. E **57**, 5707 (1996).

[3] T. S. Raju, C. N. Kumar and P. K. Panigrahi, J. Phy. A: Math. Gen. **38**, 271 (2005).

[4] V. M. Vyas, T. S. Raju, C. N. Kumar and P. K. Panigrahi, J. Phys. A: Math. Gen. **39**, 9151 (2006).

[5] S. Banerjee, E. Pavlovskaia, J. Ing and M. Wiercigroch, Int. J. Bifurcation and Chaos **20**, 3801 (2010).

[6] Y. G. Sinai, Russ. Math. Surv. **25**, 137 (1970).

[7] M. V. Berry, Annals of Physics **131**, 163 (1981).

[8] 'Chaos synchronization in Chua's circuit' by L. O. Chua, Berkeley : Electronics Research Laboratory, College of Engineering, University of California (1992).

[9] P. Muruganandam, K. Murali and M. Lakshmanan, Int. J. Bifurcation and Chaos **9**, 805 (1999).

[10] M. S. Santhanam, V. B. Sheorey and A. Lakshminarayan, Phys. Rev. E **77**, 026213 (2008).

[11] N. B. Tufillaro, T. M. Mello, Y. M. Choi and A. M. Albano, J. Physique **47**, 1477 (1986).

[12] N. B. Tufillaro and A. M. Albano, Am. J. Phys. **54**, 10 (1986).

[13] A. Heck and T. E. Meijer, Am. J. Phys. **71**, 499 (2002).

[14] A. Kini, T. L. Vincent and B. Paden, ASME J. Dynamic Systems, Measurement and Control **128**, 330 (2006).

[15] A. Okninski and B. L. Radziszewski, Differ. Equ. Dyn. Syst. **21**, 165 (2013).

[16] 'Ten lectures on Wavelets' by I. Daubechies, Society for industrial and applied mathematics, Philadelphia, Pennsylvania (1992).

[17] J. W. Kantelhardt, S. A. Zschiegner, E. K. Bunde, S. Havlin, Armin Bunde and H. E. Stanley, Phys. A **316**, 87 (2002).

[18] K. Briggs, Am. J. Phys. **55**, 12 (1987).

[19] D. Lai and G. Chen, Mathematics and Computer Modeling **27**, 1 (1998).

[20] R. Frey, 'The FFT Analyser In Mechanical Engineering Education', Instrumentation Reference Issue, Sound & Vibration (1999).

[21] P. Manimaran, P. K. Panigrahi, J. C. Parikh, Phys. Rev. E **72**, 046210 (2005) and references therein.

[22] C. K. Peng, S. V. Buldyrev, S. Havlin, M. Simons, H. E. Stanley and A.L. Goldberger, Phys. Rev. E 49, 1685 (1994).

[23] H. E. Hurst, Hydrological Sciences - Bulletin - des Sciences Hydrologiques **24**, 4 (1979).

[24] J. Feder, Fractals (Plenum, New York, 1998).

[25] T. Hwa and M. Kardar, Phys. Rev. Lett. **62**, 1813 (1989).

[26] H. J. S. Feder and J. Feder, Phys. Rev. Lett. **66**, 2669 (1991).

[27] C. Torrence and G. P. Compo, A Practical Guide to Wavelet Analysis (1998).

[28] 'A Wavelet Tour of Signal Processing', 3rd ed. by S. Mallat, Academic Press, (2008).

[29] B. B. Mandelbrot, J. W. van Ness, SIAM Rev. 10 (1968) 422; B. B. Mandelbrot, Fractals and Scaling in Finance: Discontinuity Concentration Risk, Springer Verlag, New York (1997).

[30] G. M. Le and J. L. Wang, Chin. J. Astron. Astrophys. **3**, 391 (2003).

[31] C. H. Lewenkopf and A. Müller, Phys. Rev. A **45**, 2635 (1992).

[32] V.K.B. Kota, Physics Reports **347**, 223 (2001).

[33] G. Alfano, A. M. Tulino, A. Lozano and S. Verdu, IEEE International Conference on Communication **9**, 4125 (2006).

[34] E. Kanzieper and N. Singh, J. Math. Phys. **51**, 103510 (2010).

[35] G. Basu, K. Ray, Q. M. Jonathan Wu and P. K. Panigrahi, IEEE International Conference on Systems and Informatics, 1978 (2012).